

A Low Cost Time-Resolved Raman Spectroscopic Sensing System Enabling Fluorescence Rejection

JOSEPH V. SINFIELD,* OLIVER COLIC, DANIEL FAGERMAN, and CHIKE MONWUBA

School of Civil Engineering, Purdue University, West Lafayette, Indiana 47907-2051 (J.V.S., D.F., C.M.); and Agilent Technologies, 1400 Fountain Grove Pkwy Santa Rosa, California 95403 (O.C.)

This paper describes a novel, compact, fiber-coupled, time-resolved Raman spectroscopy system that takes advantage of recent developments in diode laser and data acquisition technology to exploit the natural temporal separation between Raman and fluorescence phenomena and thereby limits the influence of fluorescence on Raman observations. The unit has been designed to be particularly low cost and is intended to provide the foundation for a wide range of in-line or fieldable sensing devices that can enhance the potential and affordability of *in situ* chemical analyses. The system operating principles, design, and performance are discussed along with its advantages and tradeoffs relative to traditional continuous wave (CW) Raman techniques. The system relies on a 6.4 kHz repetition rate 900 ps pulsed diode laser operating in the visible wavelength range (532 nm) to enhance the quality of Raman observations relative to CW and infrared systems, particularly for analytes examined in the presence of fluorophores. Time-resolved photon counting, achieved through a combination of off-the-shelf and custom hardware and software, limits the influence of fluorescence on Raman observations under pulsed excitation. The paper presents examples of the quality of Raman signatures that can be obtained with the system for a variety of compounds such as trichloroethylene, benzene, an aqueous nitrate solution, and olive oil. Further, the paper demonstrates an approximately 15-fold improvement in signal-to-noise ratio when comparing long- and short-gated time-resolved photon counting acquisition scenarios for a neat benzene sample doped with rhodamine 6G at a concentration of 1×10^{-4} M. The system's versatility and effectiveness in the assessment of complex mixtures representative of industrial or field settings is demonstrated through analysis of a gasoline sample. Additional discussion outlines how efficient signal averaging over extended observation periods can enable low concentration chemical analyses, particularly relevant in field settings.

Index Headings: Time-resolved spectroscopy; Raman spectroscopy; Fluorescence rejection; Fiber-optic probe; Photon counting.

INTRODUCTION

Raman spectroscopy is a valuable analytical technique that has seen broad application in research and industrial settings for the analysis of solids, liquids, and gases. In this technique a monochromatic light source (typically a laser) is directed toward a test specimen and inelastic photon–molecule collisions are observed. The photon–molecule collisions take place on a time scale on the order of 10^{-12} seconds. The amount of energy transferred in the collisions corresponds to the vibrational and rotational energy states of the target molecule bonds. The spectrum of observed scattered frequencies, known collectively as the Raman spectrum, thus relates to the bonds in a molecule and the relative intensity of lines in the spectrum is consistent with molecule stoichiometry. The absolute intensity of the observed scattering phenomenon, termed the Raman cross-section, is proportional to $1/\lambda^4$ (where λ = wavelength), yet the observed Raman shifts are

independent of incident wavelength since they are a function of the investigated molecule and not the wavelength of incident energy. The specificity of this phenomenon facilitates quantitative chemical analyses and enables distinction of even compounds containing the same atoms as long as they exist in different multiples or in different bond combinations.

Raman spectroscopy can be readily performed on liquids or solids, and with sufficient energy intensity, can also be applied for the analysis of gases or at marked stand-off distance¹ even through optically transparent containers. The technique is highly chemical-specific, quickly (in minutes or less) yields insight into the chemical composition of a sample, and analyzed materials require little to no preparation. Despite the method's overall merits, its use has been limited in several increasingly important contexts—such as environmental analysis, biology/biochemistry, analysis of high molecular weight compounds (e.g., petroleum fractions), emergency response, homeland security, defense, and an array of other “in-field” rather than “in-laboratory” applications—because Raman scattering is often obscured by fluorescence.

To combat fluorescence, some researchers have employed near-infrared/infrared (NIR/IR) Raman and/or Fourier transform infrared (FT-IR) Raman^{2–6} to analyze compounds for which infrared radiation does not excite the electronic state transitions that induce fluorescence. This approach, however, suffers from the $1/\lambda^4$ dependence of the Raman signal, yielding a markedly lower signal than that attainable at shorter wavelengths, limiting detection sensitivity. Further, FT-IR Raman systems are complex and costly, requiring the use of interferometric optics and often liquid helium or liquid nitrogen cooled detectors. Other researchers have attempted deep ultraviolet (UV) Raman techniques, which, while promising, require the use of a source wavelength in the sub-234 nm range to yield useful data and avoid fluorescence.⁷ This wavelength range is expensive and challenging to achieve (typically requiring high initial laser power, mode locking, and generation of multiple harmonics), resolution limiting (e.g., a 100 cm^{-1} spectral shift corresponds to over 11 nm at 1064 nm, but less than 0.5 nm if induced using 220 nm), creating a potential need for more costly instrumentation to resolve closely spaced Raman peaks, and the high energy excitation can induce unwanted fluorescence in other compounds, particularly in natural or field settings. Other researchers have attempted to capitalize upon the fact that Raman spectra are very narrow while fluorescence spectra are quite broad by employing variants of shifted excitation Raman difference spectroscopy (SERDS), in which two nearby (within ~ 2 nm) excitation wavelengths are used to interrogate a sample and the resulting spectra are subtracted from one another, effectively removing fluorescence and leaving a difference spectrum.⁸ This method is effective but requires either two lasers or a tunable source and often relies on peak fitting methods that

Received 14 April 2009; accepted 1 December 2009.

* Author to whom correspondence should be sent. E-mail: jvs@purdue.edu.

require *a priori* knowledge of likely sample constituents to define the sample Raman spectrum.

An alternate approach to limit the adverse effects of fluorescence to reap the method's analytical benefits involves application of a technique termed time-resolved Raman spectroscopy. In this method, a pulsed laser is used to interrogate the test sample. Because Raman is a scattering phenomenon and virtually instantaneous, Raman scattered photons can only exist during the laser pulse (with the notable exception of studies in granular materials in which cascading scattering may extend Raman returns beyond the incident pulse duration). In contrast, fluorescence, which occurs with a time constant on the order of 10^{-9} s, involves the absorption of a photon by atoms within the molecular structure of target compounds and subsequent emission of photons (of typically lower energy) as the atoms at an excited electronic energy state transition back to a ground state. A finite amount of time must therefore transpire between incidence and absorption of the excitation photon and emission of the fluorescence photon. Thus, Raman scattering and fluorescence emissions occur in distinctly separate time frames if excited by a non-continuous optical source approaching an impulse. This of course is a simplification, in that fluorescence induced by photons associated with the beginning of the laser pulse can start to occur before the laser pulse ends, particularly if the laser pulse approaches several nanoseconds or more in duration. However, even in this case, the photons emanating from a target sample during the very early portion of the laser pulse will likely stem from Raman scattering rather than fluorescence with significance, facilitating a marked improvement in the Raman signal-to-noise ratio (SNR) in the presence of a fluorophore relative to that achievable with a continuous wave (CW) (non-pulsed) system. While time-resolved "separation" of Raman from fluorescence has been previously demonstrated in laboratory research settings with lasers of various pulse durations and time-gated photomultiplier tube (PMT) detection,⁹⁻¹⁴ or charge-coupled device detectors (CCD),^{15,16} as well as systems with Kerr gates,^{17,18} until recently, the equipment sophistication needed for this approach has been extremely costly, impractical in all but truly state-of-the-art research settings, and cumbersome for any field or portable/mobile application.

In this context, the authors have developed a novel, compact, time-resolved Raman spectroscopy system that takes advantage of the variation in the arrival times of Raman and fluorescence photons following pulsed excitation to significantly reject fluorescence. The unit has been designed to be particularly low cost by carefully balancing incident energy characteristics, spectral resolution, detector sensitivity, and measurement time. As a result, the system can enable the use of Raman spectroscopy in a range of fluorescence-prone in-line and field settings for which the Raman technique was previously deemed to be ineffective or too costly. The following subsections of this document describe the capabilities of this unique system, noting its core advantages and tradeoffs.

PROTOTYPE SYSTEM OVERVIEW

At a fundamental level, a Raman spectroscopic system must include components to perform five key functions: sample illumination, scattered light collection, spectral separation of collected light, light detection, and signal acquisition, with all functions appropriately tailored to the nature of the target sample (e.g., solid vs. liquid, non-particulate vs. particulate,

fluorescence prone versus non-fluorescence prone) and the measurement context (e.g., laboratory vs. *in situ*, near vs. stand-off). The choice of the components used to perform each of these functions has direct implications on the performance tradeoffs of the system.

While a host of instruments exist to perform Raman analyses under a wide array of testing conditions, developments in Raman instrumentation have been most heavily focused on several key performance dimensions: illumination intensity or enhancement methods (e.g., SERS) to enhance signal strength (owing to the typically low Raman cross-section of most substances), elimination or avoidance of fluorescence interference (e.g., by the methods outlined above), speed of analysis, and spectral resolution. In terms of Raman system design, by and large this has meant that a laser is invariably chosen as the illumination source, often with a wavelength in the near- to mid-infrared range to limit the propensity for excitation and subsequent fluorescence of the sample. Further, to obtain a high flux of incident photons (and thus increase the Raman return), CW lasers are typically employed, often at power levels that achieve a balance between return signal strength and the potential to damage the sample. From a speed perspective, most modern spectroscopic systems employ a spectrophotometer or advanced Fourier techniques to present and examine a broad return spectrum that is often directed to a CCD to enable simultaneous collection of light at different wavelengths. Finally, monochromators and spectrometers have evolved to enhance spectral resolution.

In the case of the system described herein, several tradeoffs have been made to enhance performance along some dimensions while sacrificing performance along others, keeping in mind an overall goal to retain system sensitivity while limiting the effects of fluorescence, at low cost. Specifically, the system was designed with eight core components that take advantage of recent advances in diode laser, photon detection, and gating electronics technology as shown in Fig. 1. Excitation is provided using a 532 nm Q-switched microchip laser (Teem Photonics, 3 μ J/pulse energy level; <900 ps pulse duration; 6.4 kHz repetition rate) (1). The excitation source is directed through a custom beam splitter (2) to create a data acquisition trigger via a photodiode (3). Light that passes through the beam splitter is directed through a co-linear probe containing focusing optics as well as a source wavelength filter on the return light path (modified from InPhotonics) (4). The excitation source is then directed toward a sample contained within a custom chamber (5) that enables precise optical focus on a variety of test specimen forms. Scattered light is collected in a co-linear back-scatter geometry and guided into a monochromator (Oriel 77250 1/8 m, with flat-ruled 1200 lines/mm grating blazed at 500 nm) (6) and observed using a photomultiplier tube (PMT) (Hamamatsu H7422-40P) (7) operated in a photon counting mode. PMT output is observed via an impedance matched BNC link to a high-speed time digitizer (Ortec 9353) (8). For all experiments presented herein, unless stated otherwise, spectra were collected with 15 μ m slits and a 0.1 nm step size. The sample chamber and optics of the unit have been optimized for the study of liquids. However, with minor sample chamber and probe optics modifications the system can also be readily adapted for studies of solids and powders. With the exception of the free-space coupling of the laser source into the probe

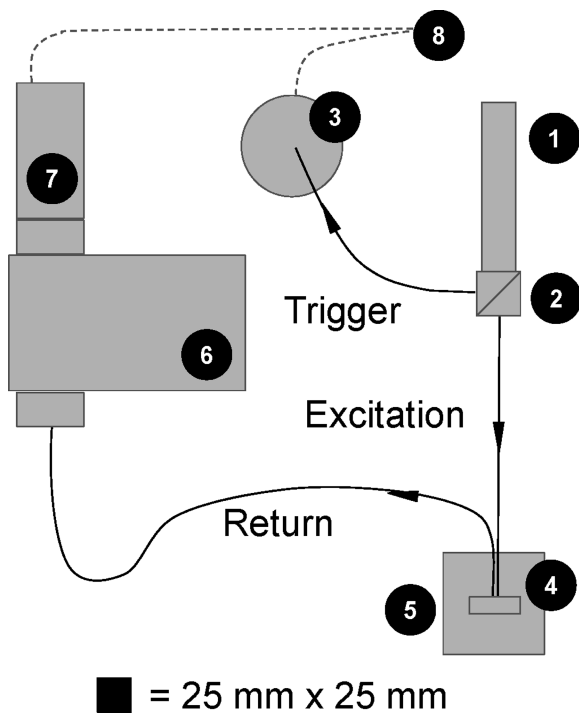


FIG. 1. Prototype Raman apparatus.

input fiber, the entire system is fiber coupled. The total cost of the prototype system as configured is approximately \$30,000.

As described, instead of making use of an infrared CW laser, the system employs a visible pulsed laser source with a duty cycle of 0.0006%/99.9994% (on for ~0.9 ns, off for ~156 000 ns). This design choice facilitates enhanced Raman intensity for a given level of input power owing to the $1/\lambda^4$ dependence of Raman intensity. Further, the pulsed laser enables time-resolved examination of the scattered return signal, prevents convolution of signals from subsequent pulses for most fluorescence samples, and thus facilitates fluorescence rejection as outlined in the Fluorescence Rejection subsection below. In addition, to limit costs, the pulsed laser has modest power but a high repetition rate, which facilitates increased SNR via signal averaging. However, this design limits the choices for return signal detection, as few, if any, devices can simultaneously collect a broad spectral output and offer sufficient time resolution to enable the analysis required to limit the influence of fluorescence on observed Raman signatures. As a result, the system trades off speed in spectral analysis. Instead of observing a broad range of wavelengths simultaneously using a detector such as a CCD, the system makes use of a monochromator and PMT to scan and examine narrow spectral bands. While relatively slow—a detailed spectrum covering 1000 cm^{-1} could take 1 to 3 hours to collect—the PMT offers rapid response time, excellent sensitivity, and can be operated in a photon counting mode with very low dark count (~300 counts/s). Further, although a “full” scan may be time consuming, in most applications, only a select number of peak locations must be examined to assess a given compound, so, in most cases, the tradeoff is very manageable. These tradeoffs are summarized conceptually in Table I and described in greater detail in the Discussion section below.

TABLE I. Comparison of traditional and prototype Raman apparatus.

Fundamental Raman system components				Attributes			
Traditional system	Lasers source	Sample	Monochromator	Detector	Data acquisition	Speed	Tradeoffs
High average power CW	Broad range of media except samples for which traditional techniques (e.g., use of NIR) still induce unwanted fluorescence (e.g., biologic samples, natural settings)	High resolution	Rapid full spectrum detection (CCD)	Continuous integration	Speed	Size	Cost
Near/mid-infrared	Broad range of media except samples containing extremely short lived (~<2 ns) fluorophores	Full spectrum/FFT	Liquid nitrogen cooled	FFT signal deconvolution	Resolution Sensitivity (via power and/or multiplex detection)	Cost Media	
Low average power Pulsed Visible		“Low” resolution Scanning spectral coverage	Slow monochromatic detection (PMT) Thermo-electric cooling	Time-resolved photon counting	Size/portability Media flexibility Affordability VIS enhanced signal [$1/\lambda^4$]	Speed Resolution	

SYSTEM OPERATION AND PERFORMANCE

To enable a discussion of the system operating principles and performance, it is important to first define several key terms that are used to characterize the output of the system. When using a time-resolved Raman instrument, the system output can be examined in three dimensions: intensity, wavelength (a function of Raman shift), and time. Intensity refers to the magnitude of the observed signal, here in the form of photon counts (the counting scheme is described in detail in the Photon Counting subsection below). The wavelength refers to the spectral region observed, and in the context of Raman observations, is typically reported in units of inverse centimeters (cm^{-1}) to indicate the frequency shift of the observed photons relative to the incident source frequency. In general, at any given observation wavelength (or shift), photon counts are collected as a function of time following the incidence of a laser pulse at the sample. The amount of time over which counts are collected since the arrival of the pulse at the sample is referred to as the counting time. In contrast, the amount of time spent at any given output wavelength collecting counts from repeated laser pulses is called the observation time. With these definitions in mind, the following outlines the operating principles employed by the time-resolved Raman system to limit fluorescence, facilitate photon counting, and develop a Raman signature.

Fluorescence Rejection. The means by which the time difference between Raman and fluorescence phenomena is employed to improve Raman signatures of compounds acquired in the presence of fluorophores can perhaps be best discussed by conceptually examining the arrival and resulting return signal from a pulse of photons (e.g., from a laser) incident upon a sample that contains molecules that absorb light at the incident frequency and are thus prone to potential fluorescence. Assuming that the Raman response is virtually instantaneous and neglecting any time dispersion in large detection volumes or diffusely scattering samples, this process is described in four stages (see Fig. 2):

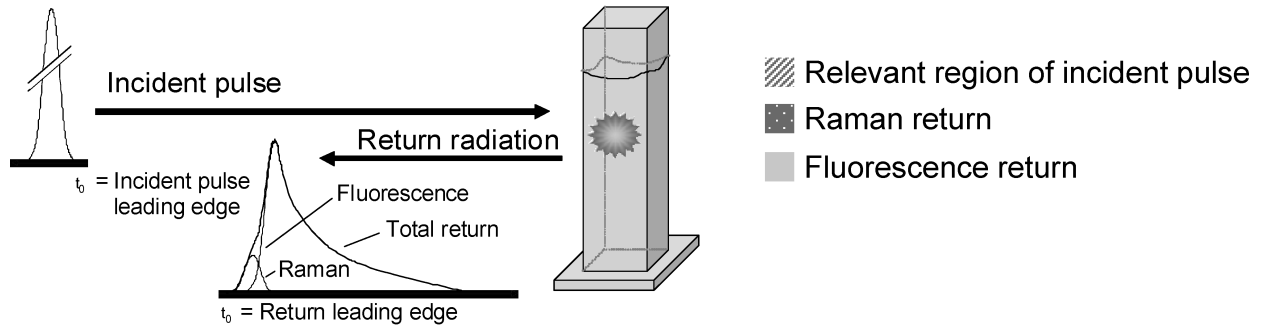
- (1) In the first stage, a subset of incident photons (i.e., the “leading edge” of the laser pulse) arrives at the sample and is scattered by the sample during a time period in which very few excited states are produced. Some of these photons are Rayleigh scattered (elastically scattered) and thus do not change in frequency. Others do change frequency based on the vibrational modes of the sample molecules and are scattered inelastically as Raman photons.
- (2) In the second stage, some subset of incident photons (still during the laser pulse if “long”) will scatter (elastically and inelastically) while fluorescence develops, but still at very low levels. Here Raman is still statistically significant relative to fluorescence (and related) emissions.
- (3) In the third stage, the “trailing edge” of the laser pulse (if “long”) is still arriving at the sample, and thus Rayleigh scattering as well as Raman is still occurring, but fluorescence and related phenomenon are also occurring at high levels, overwhelming the Raman return.
- (4) Finally, in the fourth stage, the laser pulse has ended, so there is no scattering (neither Rayleigh nor Raman), but fluorescence (and related phenomenon such as phosphorescence) still occurs until the competitive mechanisms of energy dissipation in the sample return the excited sample constituents to ground state.

In practice, these stages of optical scattering and emission are exploited by counting photons in the return radiation arriving during stages (1) and (2) that result from repeated pulses of excitation energy. With time, a significant number of Raman photon counts can be collected to build up the SNR and develop a Raman signature for the target sample.

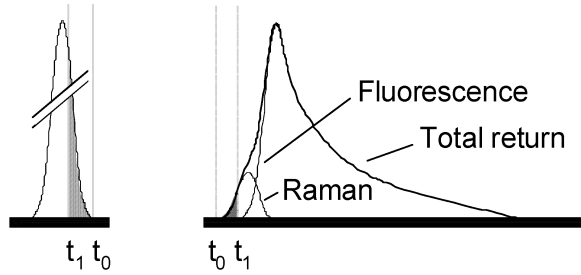
In the case of the system put forward herein, a low cost pulsed laser with a pulse duration shorter than many fluorophores is employed. The technique, of course, works equally well, if not better, as the laser pulse duration is reduced, but this increases the expense of the equipment, as fast and ultrafast pulse lasers are typically much more expensive than the laser employed here. Note that it is technically possible that a laser pulse duration longer than the fluorescence decay constant of fluorophores in a sample could be employed to carry out this same process. The key is not so much the pulse duration (as long as the return from one pulse does not overlap with the incidence of a subsequent pulse), but the time fraction of the return signal that is examined. That said, the detected Raman signal will be proportional to the laser intensity during the observation period. With longer laser pulses, only part of the laser intensity is effectively used.

The effect of this principle is illustrated in Fig. 3. Here the Raman signature of neat benzene (Fig. 3a) is contrasted with that of neat benzene doped with rhodamine 6G (Rh6G) at a concentration of 1×10^{-4} M (Figs. 3b and 3c). Note that all signatures in Figs. 3a, 3b, and 3c are plotted to the same scale to more clearly illustrate their SNR, where SNR is defined as the average peak height above the mean baseline divided by the standard deviation of the peak height, after McCreery.¹⁹ Rh6G is a known fluorophore under 532 nm excitation, with a natural fluorescence lifetime of 3.9 ns (~ 3.3 ns observed with benzene solvent). Figures 3b and 3c present the signature of the sample under 532 nm excitation at two distinct per pulse counting times to illustrate the benefits of time-resolved analysis (15 s observation time per wavelength). Figure 3b illustrates the signature observed when counts are collected from the return signal at each wavelength for a period of 8.5 ns following incidence of the laser pulse (a time at which roughly 90% of the fluorescence decay in the sample has been observed). This is effectively a “long” time gate and directionally simulates the effect of an un-gated voltage integration operation, yielding an SNR of approximately 4. Here, it is apparent that the return signature is characterized by a broad spectrum emission representative of the fluorescence signature of Rh6G and characteristic of the response that would be achieved with a CW system. In contrast, Fig. 3c illustrates the result of summing the counts from only the first 0.7 ns of the return signal resulting from each laser pulse by time gating. This signature displays the notable 996 cm^{-1} Raman peak of benzene with an SNR of approximately 62, demonstrating the system’s ability to resolve Raman peaks of a target analyte even in the presence of a fluorophore that would clearly dominate the signature of a traditional CW integrating instrument. (Note that the observed return signal is broadened mildly ($\ll 100$ ps) through the short 1/8 m monochromator and as a result of transit time spread in the PMT. Dispersion in the fiber probe is negligible given the <1.5 meter input and return fiber length. For greater fiber lengths, dispersion-compensating fiber could be employed.)

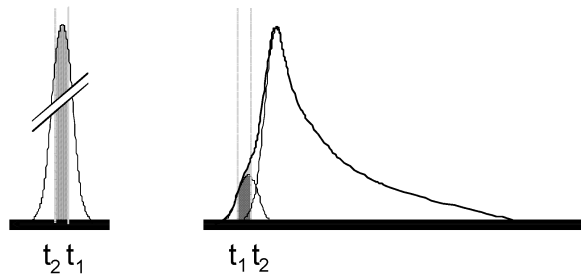
The benefit of appropriate time gating is illustrated further in Fig. 4, which highlights the result of progressively summing



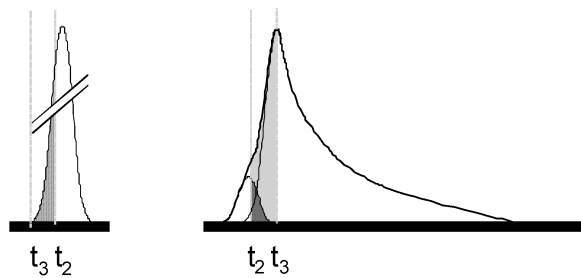
Stage 1



Stage 2



Stage 3



Stage 4

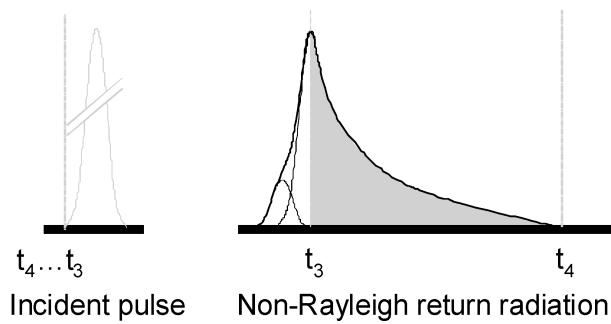


FIG. 2. Stages of incident pulse interaction with test sample.

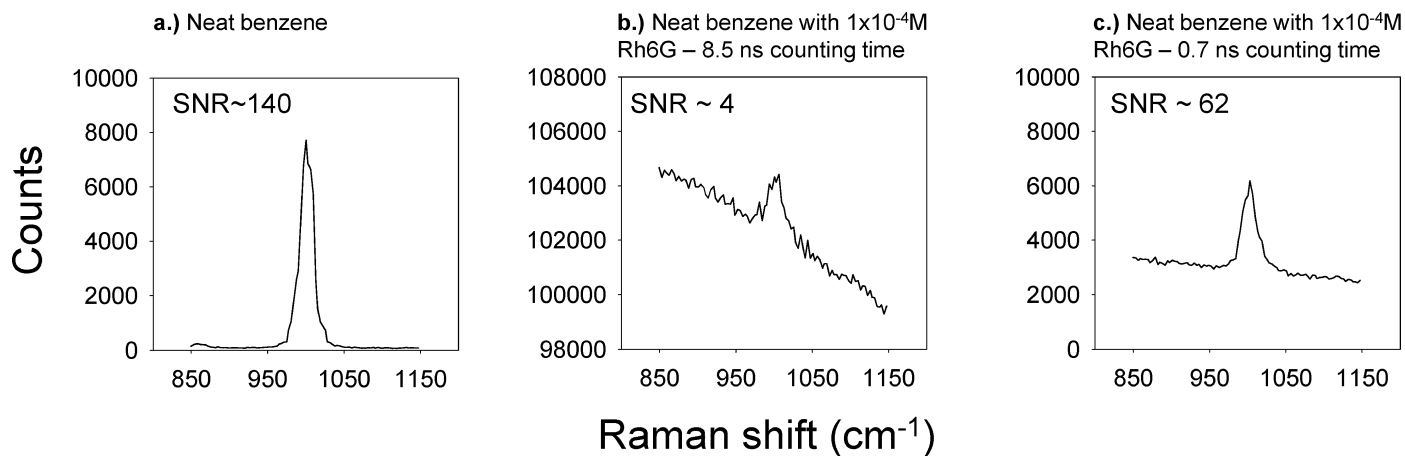


FIG. 3. Impact of time-resolved photon counting on benzene Raman signature in the presence of rhodamine 6G.

the counts in 100 ps time bins following incidence of the laser pulse at the sample. As expected, at early counting times, the signature is dominated by noise. Then, after approximately 0.7 ns, the peak SNR of the benzene 996 cm^{-1} Raman shift is achieved. The SNR then degrades again as the counting time is increased. The trend in the overall observed benzene peak Raman signature is illustrated more completely in Fig. 5 as a function of counting time.

Photon Counting. Photon counting in the system is facilitated by monitoring the output of the photomultiplier tube with a pulse-synchronized comparator-based high-speed time digitizer. After each laser pulse, a trigger signal is obtained from a photodiode positioned to capture a portion of the input beam diffracted by the beam splitter (component 2 in Fig. 1). This trigger primes a time digitizer to monitor the PMT output over a finite period of time following the laser pulse. In

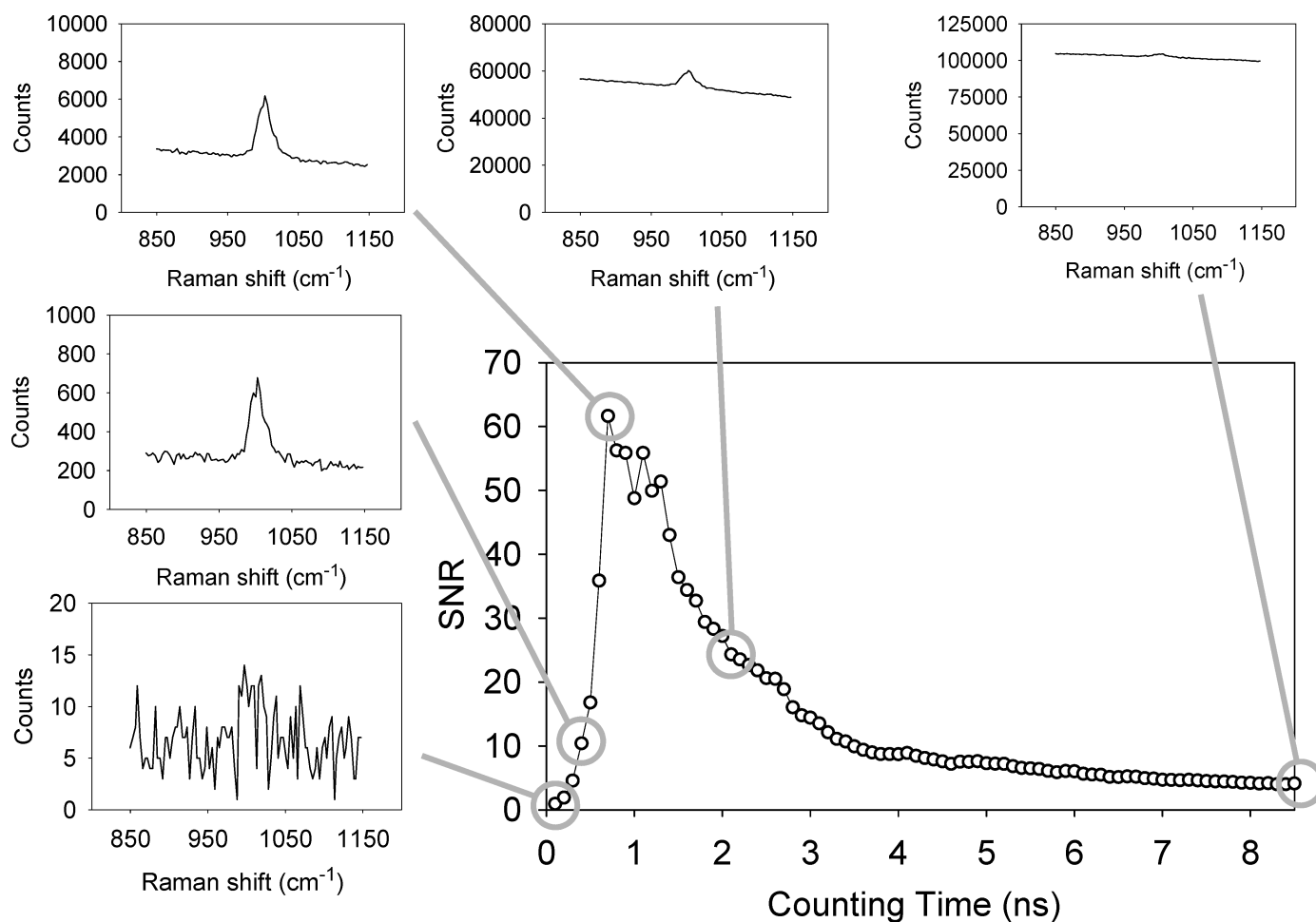


FIG. 4. Variation in neat benzene Raman peak SNR in the presence of 1×10^{-4} M rhodamine 6G as a function of counting time.

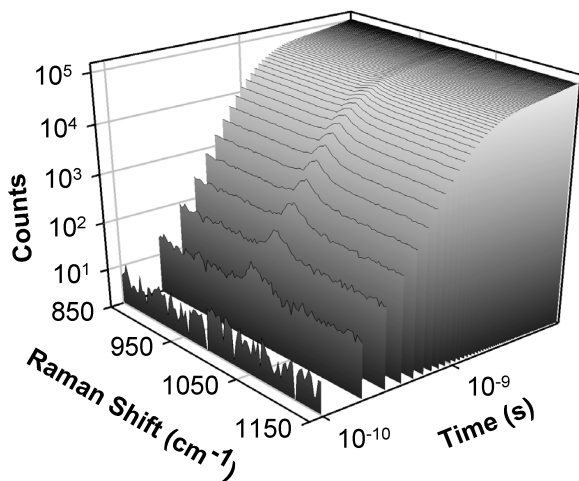


FIG. 5. Change in neat benzene Raman peak signature in the presence of 1×10^{-4} M rhodamine 6G as a function of counting time.

the case of the specific system used here, the PMT response is monitored over a series of 1000 time bins, each of 100 ps duration. Within each time bin, the PMT output is evaluated against a voltage threshold equivalent to the signal associated with approximately one photon. For the system described herein, this voltage threshold is approximately -4 mV (note that the PMT is operated with negative polarity). At the instance that the falling edge of the PMT response crosses this threshold, a count of “1” is registered in the appropriate time bin. If the PMT response does not cross the pre-defined voltage threshold, no counts will be recorded. This binary scheme limits the adverse impact of low amplitude electrical noise and PMT noise emissions that initiate after the photocathode. Noise or “false counting” is of course also reduced in the overall system by the fact that PMT monitoring is synchronized with the laser pulse, limiting the influence of random dark counts.

Given that only one voltage threshold is used in the counting algorithm, this counting approach cannot differentiate single photon returns from simultaneous (parallel) multi-photon returns. Further, the potential to observe multiple sequential counts (series) resulting from a single laser pulse is of course limited by the response time of the PMT (in this case, the H7422-40P has a rise time of ~ 1 ns), which must begin to fall before rising again to record a subsequent peak count. In practice, the PMT response can “fall and rise” through a one photon equivalent voltage threshold in 2 to 3 ns, depending on the exact shape of the PMT output. Despite these limitations, over many laser pulses, significant numbers of counts from the return radiation can be accumulated in the time digitizer bins to create a histogram of counts vs. time since the trigger (for a given observed spectral band). (Note that a similar data set can be obtained by monitoring the PMT output using a high speed digital oscilloscope configured to create a histogram of peak hits in a defined time versus voltage space, but at substantially greater cost than can be achieved using a for-purpose time-digitizing comparator circuit).

Raman Signature Development. The counts recorded with the time-digitizing comparator can be used to develop the Raman signature of a compound by summing counts in the early time bins at each spectral band observed. The bins used in the summation include those that mark the onset of Raman return (a function of the transit distance of the system, lag in

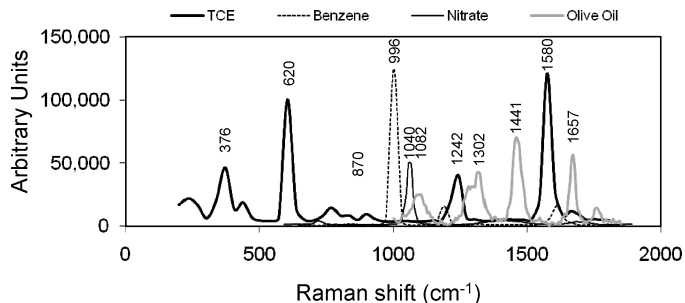


FIG. 6. Representative Raman signatures obtained with prototype time-resolved apparatus.

electrical response, and any intentional delay incorporated in the circuitry) to those denoting the point at which fluorescence counts begin to degrade the Raman SNR. This latter cutoff is a function of the decay constant of the fluorophore(s) present in the target medium as this will define the time at which fluorescence photons will overwhelm the Raman return (the transition from stage 2 to stage 3 described above). In practice, the sum of the counts within the defined set of time bins (again, referred to as the “counting time”) can be calculated for each spectral band observed to create a Raman signature in terms of signal counts versus Raman shift (cm^{-1}). Including the counts from only early time bins will result in a signal likely dominated by noise (see Fig. 5, early counting times). In contrast, including counts from “late” time bins in the counting will result in a signature dominated by fluorescence (assuming a fluorophore is present) (see Fig. 5, late counting times). Thus, the time bins that are to be examined in the signal must be selected carefully. For any given test scenario, the signature for a “counting time” corresponding to the sum of bins i through j can be compared to the signature achieved by summing bins i through $j + 1$, and so on, to assess the resulting change in SNR for target Raman peaks and select the optimal counting time, which should remain constant for any given fluorophore system.

Figure 6 illustrates the quality of Raman signatures that can be obtained with the system, highlighting its versatility. The thick solid line illustrates the Raman signature of trichloroethylene (TCE), a common chlorinated solvent, with notable peaks at 376 (δ skeletal), 626 (νCCl), 1242 (δCH), and 1580 cm^{-1} ($\nu\text{C}=\text{C}$). The dotted spectrum reflects the signature of benzene (996 cm^{-1} , $\nu(\text{CC})$ ring stretch), a fuel constituent and common environmental pollutant. The thin solid line highlights nitrate (note distinct Raman line at 1040 cm^{-1} , (νNO) symmetric stretch) as a constituent of a 8.1×10^{-2} M aqueous solution of ammonium nitrate (NH_4NO_3), which is common in fertilizers. Finally, the gray line depicts the Raman signature of olive oil, with peaks at 1082 (νCC), 1302 (δCH -twist), 1441 (δCH -shear), and 1657 cm^{-1} ($\nu\text{C}=\text{C}$). All signatures presented here were acquired with a 30 s observation time per wavelength except for the olive oil, which was analyzed for 240 s at each wavelength.

DISCUSSION OF SYSTEM ADVANTAGES AND TRADEOFFS

Few analytical instruments can claim the versatility of a Raman apparatus in terms of the potential to quantitatively assess the chemical composition of a broad range of materials, particularly with little to no sample preparation (and at the cost

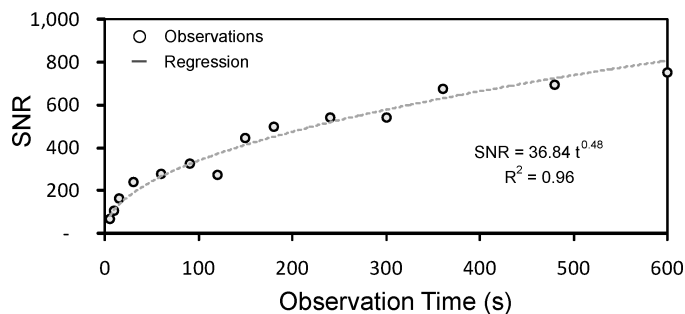


FIG. 7. Effect of observation time on SNR.

point of the time-resolved Raman system presented here). Raman is of course applicable to any compounds exhibiting Raman active vibrational modes, which comprises the vast majority of diatomic and polyatomic molecules. Further, the range of energy associated with any given vibrational mode of a molecule (which is directly related to the bandwidth of the Raman line) is inherently narrow, which can often allow ready distinction of compounds present in multi-component substances. In very complex systems, there is the potential for Raman bands to overlap, partially or completely. However, Raman intensities are also tied to molecular stoichiometry, and thus the signatures of multi-component systems are a superposition of the signatures of the system's constituents. While not always straightforward to decouple, multiple researchers have successfully applied partial least squares or principal component analysis to quantitatively assess constituents in complex substances.^{2,20–22}

Beyond these benefits, which apply to any Raman system, the versatility of the particular time-resolved Raman system presented here balances performance in several unique ways as described below.

Efficient Signal Averaging to Enable Low Concentration Chemical Analyses. By operating with a voltage threshold to discriminate photon counts from noise, and at kHz repetition rates, the system has excellent sensitivity and potential to rapidly acquire high SNR Raman signatures even from samples containing low concentrations of target compounds. Since photon counting is effectively a “digital” process—count = 1, no count = 0—increases in observation time provide an opportunity to capture photons from very low concentration samples while effectively rejecting noise from both electrical interference (of a magnitude typically below the voltage threshold established to define a count) and asynchronous dark counts. Effectively, the counts from multiple laser pulses can be accumulated over time to improve SNR, although shot noise will ultimately limit achievable benefits.

For the prototype system the SNR improves with approximately the square root of observation time, with the benefit of increased observation time declining significantly beyond 240 s. This point is illustrated in Fig. 7, which presents the results of tests on neat benzene conducted to monitor SNR as a function of observation time. Each point in the figure represents the average SNR from five observations of the Raman peak representing ring stretching in benzene (996 cm^{-1}) (see, for example, Fig. 3a).

While observations of duration greater than 240 s will indeed increase SNR, the increase is small with respect to the time needed to achieve significantly higher SNR values. So, to optimize test time and SNR, scans with the system are typically

carried out for 240 to 300 seconds when high sensitivity is required. Successful quantitative analyses have been performed to date using this counting approach on a variety of compounds including aqueous solutions of nitrate down to 2 ppm concentration, chlorinated solvents such as tetrachloroethene down to 150 ppm, and fractional analyses of fatty acids in vegetable oils.

Amenability to Circumstances Involving Fluorophores. As discussed in detail above, due to the short pulse excitation source and GHz time-gating data acquisition circuitry, Raman signals can be effectively acquired in a time interval prior to the onset of significant fluorescence emission without deconvolution algorithms. This capability opens the door to low cost application of Raman analytics in fluorescence prone environments that limit the effectiveness and/or sensitivity of CW systems, even if operating in the NIR.

Balance of Sensitivity and Resolution. By operating at 532 nm in the visible range of the optical spectrum, the prototype Raman sensor balances the inevitable tradeoffs that must be made between Raman signal intensity and peak resolution while limiting the potential to cause fluorescence in many compounds. This provides two key benefits: (1) enhanced Raman cross-section, and (2) improved Raman peak resolution in complex samples.

Enhanced Raman Cross-Section: Operating at 532 nm, the prototype system offers a 16-fold and 4.7-fold advantage in Raman signal intensity over 1064 nm and 785 nm systems (traditionally used to limit fluorescence), respectively, due to the $1/\lambda^4$ dependence of the Raman cross-section, potentially revealing features of low concentration constituents not prevalent in traditional infrared analyses. While it is acknowledged that further shifts toward the UV could provide preferable signal intensity without excessive fluorescence, sub-nanosecond pulsed laser sources at wavelengths shorter than 532 nm are not yet commercially available at comparable costs.

Improved Raman Peak Resolution in Complex Samples: Use of a 532 nm source permits resolution of Raman peaks separated by as little as 17 cm^{-1} using low cost 0.5 nm resolution spectrometers (versus $\sim 70\text{ cm}^{-1}$ using deep UV). With increasing sample complexity (e.g., solutions containing multiple unknowns), more Raman peaks will be present and this advantage could yield deeper compositional insight at low cost.

Fieldable Versatility. The Raman system design presented here also provides an excellent foundation for fieldable or portable sensing devices based on several key attributes:

Compact Fiber-Coupled Design: The fiber-coupled design of the sensor provides great flexibility in system configuration and physical footprint with total hardware volume amounting to less than 0.1 m^3 .

Potential for Noncontact Assessment: Because Raman spectroscopy makes use of a focused laser source, there is the potential to evaluate target compounds through a protective optically transparent window, facilitating the development of a robust device that can be effectively protected from the elements while in use outdoors or in harsh industrial locations.

Low Cost: The system makes use of both custom and commercially available components and, with a prototype cost

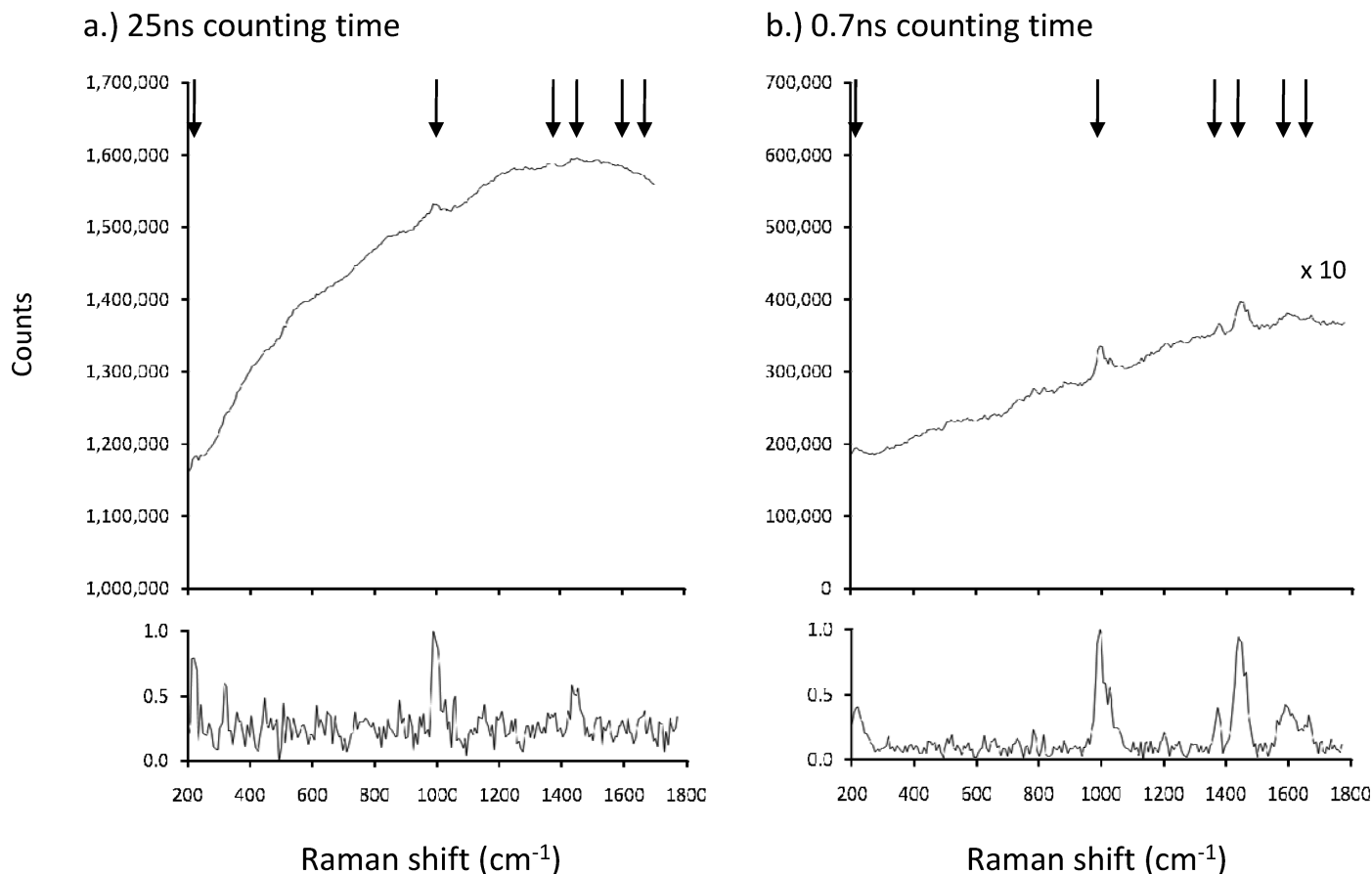


FIG. 8. Effect of counting time on Raman signature of gasoline: (a) 25 ns counting time, (b) 0.7 ns counting time.

under \$30,000, is substantially less expensive than comparable traditional instruments capable of fluorescence rejection.

Combined, these advantages offer potential for excellent versatility, sensitivity, and analytical specificity compared to existing instruments of similar scale and cost. The versatility of the system for practical field and industrial measurements is exemplified in Fig. 8, which presents the results of a time-resolved scan of high octane gasoline (240 s observation time per wavelength, 15 μm slits, 0.2 nm step size), a complex mixture containing multiple compounds that fluoresce under 532 nm excitation and have varying fluorescence lifetimes ranging from several nanoseconds to tens of nanoseconds. Figures 8a and 8b present the Raman signatures captured at counting times of 25 ns (again a time at which roughly 90% of the fluorescence decay in the sample has been observed) and 0.7 ns, respectively. In both panels, the upper signature presents the actual counts acquired over the stated counting period (noting that the counts for the 0.7 ns signature have been multiplied by 10 to facilitate visual comparison) and the lower curve illustrates the signature obtained when the fluorescence and/or background is removed and the result is normalized by the intensity at the benzene 996 cm^{-1} shift. Comparing the upper curves in the two sets of data, it is apparent that the shorter counting time yields a much flatter signature showing markedly less influence from fluorescence. This advantage significantly reduces the complexity and increases the reliability of background subtraction, which is quite difficult to perform on the 25 ns data. It is also apparent by comparing the normalized signatures that the SNR

of the 0.7 ns signal is superior to that at 25 ns. The 0.7 ns signature clearly displays the 996 cm^{-1} $\nu(\text{CC})$ ring-stretch of benzene as well as the 1380 cm^{-1} $\delta(\text{CH})$ -twisting and 1450 cm^{-1} $\delta(\text{CH})$ -wagging lines of heptanes. Additional lines in the 220–245 cm^{-1} region, and in the 1580–1650 cm^{-1} region, are also visible, likely representing the LAM-mode of decane and $\nu(\text{C}=\text{C})$ stretching in olefins, respectively. In contrast, several of the Raman lines (e.g., 1380, 1580–1650 cm^{-1}) are barely visible at 25 ns and the other notable peaks are significantly reduced. Overall, this example demonstrates the merit of the time-resolved technique when investigating complex, fluorescence prone samples typical of industrial or field settings.

CONCLUDING REMARKS

This paper has introduced a low cost (<\$30,000), high sensitivity prototype Raman system that puts Raman spectroscopy in reach for a broad range of users and applications. The system relies on a kHz repetition rate laser operating in the visible wavelength (532 nm) range to enhance the quality of Raman observations relative to CW and infrared systems, particularly for analytes examined in the presence of fluorophores. Time-resolved photon counting, achieved through the use of a combination of low cost off-the-shelf and custom components, limits the influence of fluorescence on Raman signatures by taking advantage of the fact that Raman and fluorescence phenomena occur in distinct time frames.

The paper presents examples of the quality of Raman signatures that can be obtained with the system for a variety of

compounds and discusses how efficient signal averaging over extended observation periods can enable low concentration chemical analyses.

The low cost and compact fiber-coupled design of the system could facilitate its use in a variety of industrial and field settings. In particular, the device provides the foundation for analytical instrumentation targeted toward multiple unique sensing challenges, including:

- (1) Observations of Raman signatures in fluorescence prone systems such as biochemical analyses, pharmaceutical quality control, and petroleum fraction assessment in refining.
- (2) Real-time and long-term monitoring for environmental pollutants in natural settings likely to involve humics, fulvics, or microorganisms that tend to fluoresce, including the assessment of run-off from agricultural operations and studies of contaminants in soils with fluorescence-susceptible mineralogy.
- (3) Portable and fieldable instrumentation for emergency response, homeland security, and defense, which must provide rapid chemical analysis among complex chemical backgrounds and natural or anthropogenic fluorophores.

ACKNOWLEDGMENTS

The authors would like to thank DICKEY-john Corporation and Purdue University's Discovery Park Center for the Environment for supporting the work presented in this study. The authors are also particularly grateful to Dr. Dan Logue and Ron Steffen of DICKEY-john Corporation for their continuous technical support and critical review of the work carried out in this effort.

1. S. K. Sharma, A. K. Misra, and B. Sharma, *Spectrochim. Acta, Part A* **61**, 2404 (2005).

2. J. B. Cooper, P. E. Flecher, T. M. Vess, and W. T. Welch, *Appl. Spectrosc.* **49**, 586 (1995).
3. M. B. Seasholtz, D. D. Archibald, A. Lorber, and B. R. Kowalski, *Appl. Spectrosc.* **43**, 1067 (1989).
4. J. B. Cooper, K. L. Wise, W. T. Welch, M. B. Sumner, B. K. Wilt, and R. R. Bledsoe, *Appl. Spectrosc.* **51**, 1613 (1997).
5. H. Shinohara, Y. Yamakita, and K. Ohno, *J. Mol. Struct.* **442**, 221 (1998).
6. K. J. Johnson, R. E. Morris, and S. L. Rose-Pehrsson, *Energy Fuels* **20**, 727 (2006).
7. L. C. T. Shoute, K. J. Schmidt, R. H. Hall, M. A. Webb, S. Rifai, P. Abel, P. H. Arboleda, A. Savage, J. T. Bulmer, and G. R. Loppnow, *Appl. Spectrosc.* **56**, 1308 (2002).
8. J. Zhao, M. M. Carrabba, and F. S. Allen, *Appl. Spectrosc.* **56**, 834 (2002).
9. P. P. Yaney, *J. Opt. Soc. Am.* **62**, 1297 (1972).
10. R. P. Van Duyne, D. L. Jeanmaire, and D. F. Shriver, *Anal. Chem.* **46**, 213 (1974).
11. J. M. Harris, R. W. Chrisman, F. E. Lytle, and R. S. Tobias, *Anal. Chem.* **48**, 1938 (1976).
12. S. Burgess and I. W. Shepherd, *J. Phys. E: Sci. Instrum.* **10**, 617 (1977).
13. K. Kamogawa, T. Fujii, and T. Kitagawa, *Appl. Spectrosc.* **42**, 248 (1998).
14. J. Howard, N. J. Everall, R. W. Jackson, and K. Hutchinson, *J. Phys. E: Sci. Instrum.* **19**, 934 (1986).
15. D. V. Martyshev, R. C. Ahuja, A. Kudriavtsev, and S. B. Mirov, *Rev. Sci. Instrum.* **75**, 630 (2004).
16. E. V. Efremov, J. B. Buijs, C. Gooijer, and F. Ariese, *Appl. Spectrosc.* **61**, 571 (2007).
17. N. Everall, T. Hahn, P. Matousek, A. W. Parker, and M. Towrie, *Appl. Spectrosc.* **55**, 1701 (2001).
18. P. Matousek, M. Towrie, C. Ma, W. M. Kwok, D. Phillips, W. T. Toner, and A. W. Parker, *J. Raman Spectrosc.* **32**, 983 (2001).
19. R. L. McCreery, *Raman Spectroscopy for Chemical Analysis* (Wiley-Interscience, New York, 2000), 1st ed., p. 49.
20. M. J. Goetz, Jr., G. L. Cote, R. Erckens, W. March, and M. Motamedi, *IEEE Trans. Biomed. Eng.* **42**, 728 (1995).
21. N. K. Afseth, V. H. Segtnan, B. J. Marquardt, and J. P. Wold, *Appl. Spectrosc.* **59**, 1324 (2005).
22. Y. Oshima, Y. Komachi, C. Furihata, H. Tashiro, and H. Sato, *Appl. Spectrosc.* **60**, 964 (2006).